Surface Science 603 (2009) 2294–2299

Contents lists available at ScienceDirect

Surface Science

journal homepage: www.elsevier.com/locate/susc

Stabilization of bimolecular islands on ultrathin NaCl films by a vicinal substrate

M.E. Cañas-Ventura [a,b,1], W. Xiao [a,2], P. Ruffieux [a], R. Rieger [c], K. Müllen [c], H. Brune [b], R. Fasel [a,*]

[a] Empa, Swiss Federal Laboratories for Materials Testing and Research, nanotech@surfaces Laboratory, Feuerwerkerstrasse 39, 3602 Thun, Switzerland
[b] Institut de Physique de Matière Condensée, Ecole Polytechnique Fédérale de Lausanne, Station 3, 1015 Lausanne, Switzerland
[c] Max-Planck-Institut für Polymerforschung, Ackermannweg 10, 55128 Mainz, Germany

ARTICLE INFO

Article history:
Received 30 September 2008
Accepted for publication 6 May 2009
Available online 23 May 2009

Keywords:
Scanning tunnelling microscopy (STM)
Molecular self-assembly
Insulating ultrathin films
Selective hydrogen bond
NaCl
Vicinal single crystal surfaces
Gold

ABSTRACT

The structure of ultrathin NaCl films on Au(1 1 1) and on Au(11 12 12), as well as the one of bimolecular 3,4,9,10-perylenetetracarboxylic diimide (PTCDI) and 1,4-bis-(2,4-diamino-1,3,5,-triazine)-benzene (BDATB) islands on NaCl films on both surfaces have been studied with a low-temperature scanning tunnelling microscope. We show that intermixed bimolecular assemblies based on selective three-fold hydrogen-bonding (H-bonding), that have previously been observed on Au(1 1 1) and on Au(11 12 12), can also be stabilized on insulating NaCl films on Au, however, only if these films are grown on Au(11 12 12) and not on Au(1 1 1). The behaviour of the heterocomplex structures is found to be largely influenced by the structural properties of the underlying substrate and by the number of NaCl layers. On a partly NaCl-covered Au(1 1 1) surface, the excess of molecules after completion of the first layer on Au prefers to form a second molecular layer based on ordered heterocomplex structures rather than to adsorb on the NaCl islands. The use of a vicinal surface together with the strong cohesion characteristic of the NaCl film introduces smooth elastic deformations on the NaCl(0 0 1) plane. As a consequence, the periodically modified structure of the overlayer provides preferential binding sites and allows adsorption of two-dimensional molecular structures. In contrast to what is observed on Au(11 12 12), the molecular domains on the NaCl film do not follow the Au step directions, but the NaCl(0 0 1) high symmetry directions. Our results provide a strategy to increase the adsorption energy of flat molecules on insulating layers by choosing a vicinal metal substrate.

1. Introduction

The controlled formation of functional supramolecular assemblies on insulating substrates is of great interest, not only because of the potential implementation of such systems to molecular electronics, but also from a fundamental point of view. At the adsorbate–metal interface several physical and chemical phenomena such as hybridization [1] and charge transfer [2] may strongly affect the behaviour of the adsorbed molecular entities. New strategies to tune the characteristics of the adsorbate–surface interface are thus intensively explored [3], but only few studies have examined the directly related consequences on the electronic properties of the molecular adsorbates themselves. Among the strategies to tune the properties of organic–inorganic (adsorbate–surface) interfaces, the use of ultrathin insulating layers between a metallic surface and the molecular adsorbates is one of the most prominent. The reason for that is a combination of (1) the efficient decoupling of the molecular electronic structure from the one of the substrate, and (2) the possibility of using scanning tunnelling microscopy (STM) to probe the local properties of molecular adsorbates also on insulating ultrathin films, since they allow tunnelling into the underlying metal. Ultrathin metal oxide layers have been used to reduce the electronic interaction between molecules and substrates allowing the observation of fluorescence [4], vibronic states [5], and charging of isolated molecules [6]. Franke et al. have recently reduced the electronic coupling of C_{60} with a metal surface by locking and lifting each fullerene with a second molecular species [7]. Furthermore, it has been shown that, upon adsorption of molecules on ultrathin NaCl films on metal surfaces, inherent electronic and optical properties of *individual molecules* can be studied [8–10]. However, to our knowledge, there are only three published STM studies on the growth of *two-dimensional molecular islands* on insulating NaCl layers, two of them on metal-containing porphyrine molecules [11,12], and the third one on C_{60} molecules [13]. The small number of investigations about adsorbates on NaCl layers is at least partly due to weak molecule–substrate interactions, which make the stabilization and STM imaging of such systems a challenging task. We present a strategy increasing the molecule–NaCl binding energy while maintaining the structure of

* Corresponding author. Tel.: +41 044 823 4348; fax: +41 044 33 228 6465.
E-mail address: roman.fasel@empa.ch (R. Fasel).
[1] Present address: Kamerlingh Onnes Laboratory, Leiden University, P.O. Box 9504, 2300 RA Leiden, The Netherlands.
[2] Present address: Nanoscale Physics and Devices Laboratory, Institute of Physics, Chinese Academy of Sciences, P.O. Box 603, Beijing 100190, PR China.

0039-6028/$ - see front matter © 2009 Elsevier B.V. All rights reserved.
doi:10.1016/j.susc.2009.05.007

the molecular domains identical to the ones formed directly on metal substrates.

Recently, we reported on the formation of regular 3,4,9,10-perylenetetracarboxylic diimide (PTCDI) and 1,4-bis-(2,4-diamino-1,3,5,-triazine)-benzene (BDATB) bimolecular wires and ribbons based on a hydrogen-bonding motif (Fig. 1) on Au(1 1 1) and on the vicinal Au(11 12 12) surface [14]. The experiments demonstrated the formation of three-fold hydrogen bonds between complementary molecular end groups on both surfaces. Furthermore, the equidistant and parallel steps on the Au(11 12 12) surface were shown to guide the bimolecular rows along the steps: at coverages between 0.1 and 0.2 monolayers (ML, defined as the saturation coverage of the first layer), parallel and equally spaced single- and double-row bimolecular wires are formed over extended length scales. If ever such structures were to be implemented as part of a molecular electronic device, they would need to be electronically decoupled from the underlying surface. Therefore the controlled formation of a particular supramolecular structure on insulating substrates while maintaining its structure is an important step in this direction.

Here we report on the formation of PTCDI–BDATB bimolecular ribbons on the NaCl/Au(1 1 1) and NaCl/Au(11 12 12) surfaces. The behaviour of the supramolecular structures with respect to the NaCl islands strongly depends on the underlying metal substrate, even though the overall structure of the NaCl(0 0 1) layers is the same in both cases. A comparative analysis of results obtained on the flat and the vicinal surfaces shows that the molecular adsorption energy on NaCl strongly increases on the vicinal surface and thereby opens a new strategy to stabilize two-dimensional molecular islands on ultrathin NaCl layers.

2. Experimental procedures

STM experiments were performed in an ultra high vacuum (UHV) chamber (base pressure of 2×10^{-10} mbar) housing sample preparation facilities and a low-temperature STM (LT-STM) from Omicron GmbH. Sample cleaning was performed by standard sputter-annealing methods for Au(1 1 1) and Au(11 12 12). NaCl was deposited by sublimation from a salt loaded quartz crucible heated to 670 K. The deposition rate was monitored by a quartz microbalance. Both molecular species, PTCDI (99+%, Fluka Chemie GmbH) and BDATB (synthesized by the co-authors at MPIP Mainz), were sublimated onto either NaCl/Au(1 1 1) or NaCl/Au(11 12 12) substrates kept at room temperature (RT). STM experiments were performed at 70 K in the constant current mode using either a mechanically cut Platinum–Iridium (Pt–Ir) tip or a chemically etched Tungsten (W) tip. Voltages indicated for STM images correspond to sample bias. STM data have been analyzed using the WSxM software [15].

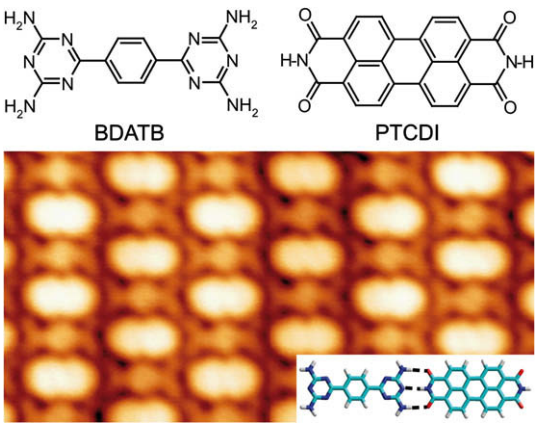

Fig. 1. Chemical structure of BDATB and PTCDI. The STM image (11×5 nm^2) shows the alternating arrangement of BDATB and PTCDI molecules on Au(1 1 1). The same structure is observed, and has been reported [14] on Au(11 12 12). Inset: three-fold H-bond formed between the complementary end groups of BDATB and PTCDI.

3. Results and discussion

3.1. Growth of NaCl on the Au(1 1 1) surface

The growth of ultrathin NaCl films and their properties have been characterized by STM on several metal and semiconductor surfaces such as Ge(1 0 0) [16], Al(1 1 1) and Al(1 0 0) [17], Cu(1 1 1) [18], Cu(2 1 1) [19], Cu(3 1 1) [20], Cu(5 3 2) [21], Ag(1 0 0) and Ag(1,1,19) [22], but to our knowledge no study of the growth of ultrathin NaCl films on Au(1 1 1) has been reported. Before studying the adsorption of molecules on the NaCl layers, we thus investigated the growth of NaCl on Au(1 1 1) and on Au(11 12 12) [for Au(11 12 12), see Section 3.3].

After a deposit of NaCl with the Au(1 1 1) sample held at 180 K, STM images show that large areas of the surface are NaCl-free, and that NaCl islands preferentially nucleate at step edges (Fig. 2a). NaCl islands present a characteristic square shape with kinks. Atomically resolved images show that they exhibit a (0 0 1) surface termination. Different apparent heights are measured for the NaCl islands, which indicate the formation of double [2 ML NaCl, (2.8 ± 0.2) Å] and triple [3 ML NaCl, (4.0 ± 0.2) Å] layers before completion of the first monolayer [1 ML NaCl, apparent height (1.8 ± 0.2) Å] [23]. The characteristic straight edges of the NaCl islands are due to island borders coincident with the apolar axes of the NaCl crystal (see scheme in Fig. 2c). This structure thus seems to minimize the total energy for both, 1 ML NaCl islands with local dipoles oriented parallel to the surface and 2 ML NaCl islands with dipoles parallel and perpendicular to the surface. At the coverage in Fig. 2, the third layer appears as small clusters. With increasing coverage, the 3 ML NaCl adislands grow as well with straight apolar edges. NaCl thin film growth proceeds by nucleation of islands and their subsequent growth. Under the conditions used here, second layer nucleation takes place before completion of the underlying layer leading to a three-dimensional growth morphology. We have attempted the formation of complete layers by grazing incidence ion bombardment of the sample after NaCl deposition. The ion bombardment seemed to remove some of the additional NaCl adislands, but results were not conclusive.

The herringbone reconstruction geometry of the underlying Au(1 1 1) surface is unaltered, giving rise to an apparent herringbone-like topography on the NaCl islands. Within the error bar the corrugation of the partial dislocations of the Au(1 1 1) – ($\sqrt{3} \times 22$) reconstruction is identical to the one on 1 and 2 ML NaCl islands. The orientation of NaCl layers in the middle of large gold terraces does not appear to be correlated with the one of the atomic Au(1 1 1) lattice or with the herringbone superstructure. However, islands close to steps have their apolar axes oriented parallel to the steps. Since for the Au(1 1 1) surface the steps are only locally straight, the NaCl adlayer adapts in order to get as close as possible to an overall favourable orientation.

The lattice constant of the NaCl islands, as determined from high resolution STM images from both, single- and double-layer islands, varies from (5.0 ± 0.2) Å to (5.4 ± 0.2) Å, depending on the distance between the measurement location and the nearest step edge(s) (on the flat terrace, and at least five atomic rows away from the step edge position), and the straightness of the step. These values correspond to a compression of (10.8 ± 3.6)% to (4.1 ± 3.6)% with respect to the bulk NaCl lattice constant of 5.63 Å. Gradual accommodation of the NaCl lattice over monatomic steps is observed to take place by several unit cells with different lattice

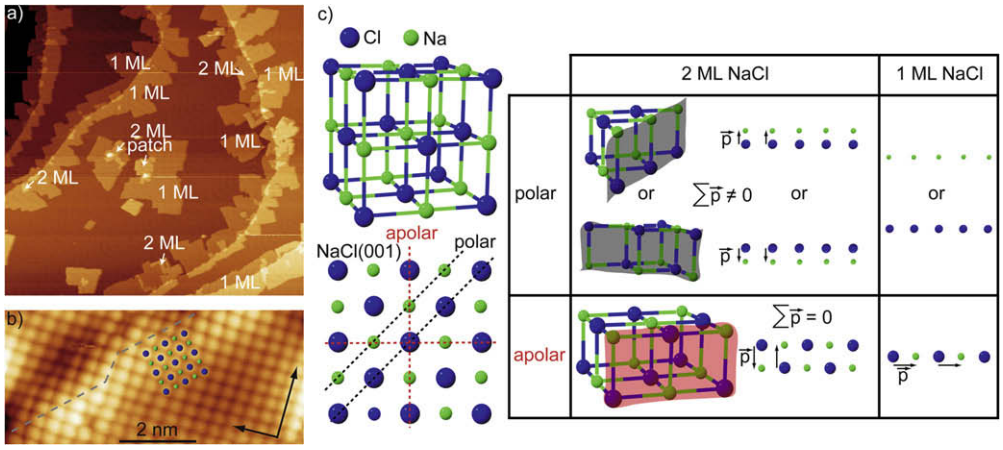

Fig. 2. (a) and (b) STM images of the surface topography resulting from deposition of NaCl on Au(1 1 1) at 180 K. (a) Steps act as nucleation sites for the growth of straight-edged NaCl islands. Although the first NaCl layer is not completed, 2 ML domains are already formed (300 × 300 nm^2). (b) Atomic resolution STM image showing a double-layer NaCl island crossing an irregular step of the underlying Au surface (dashed grey line). Both polar directions are indicated by black arrows ($V = -2.5$ V, $I = 0.05$ nA). Calculations of the local density of states attribute the protrusions observed by STM to the Cl^- anions [24], as indicated by the superposed model. (c) NaCl crystal structure and schemes defining polar and apolar axes, as well as polar and apolar 1 ML and 2 ML NaCl island edges.

constants forming an elastic "carpet" across the steps. The most interesting aspect of this growth behaviour is that the presence of steps does not lead to dislocations and therefore one NaCl island crosses several steps while staying a single crystallographic domain. This well-known carpet-like overgrowth of steps, kinks, and defects [24] is due to strong internal cohesion of the film, which avoids misfit dislocations in the NaCl layer (see Fig. 2b, where a dashed grey line indicates the estimated step edge position). The suggested mechanism is that the epitaxial NaCl layer avoids strong Coulombic forces by a smooth elastic deformation in the regions near the steps, instead of forming a sharp step.

3.2. Bimolecular deposit on NaCl/Au(1 1 1)

We now turn to the molecular structures obtained by codeposition of BDATB and PTCDI on the above described NaCl islands on Au(1 1 1). The relative abundance of molecules will be used to qualitatively compare adsorption energies on the bare metal and on 1, 2, and 3 ML NaCl islands. STM images taken after the deposition of molecules show an insignificant amount of molecules adsorbed on the 2 ML thick NaCl film (Fig. 3a). A schematic identification of the observed features is given in the line profile. When the metal surface is completely covered by a mixture of bimolecular and 2 ML NaCl islands, few molecules are adsorbed on the NaCl islands (Fig. 3b). However, a detailed analysis of the STM images reveals that these molecules are not adsorbed on top of the 2 ML NaCl film, but located within 1 ML deep vacancy islands (see line profile in Fig. 3b). Therefore, we conclude that molecules do not adsorb on perfect NaCl, but are trapped by defects. Increasing the coverage leads to preferential adsorption on top of the first layer of molecules rather than on the NaCl islands.

From these results, the following adsorption energy hierarchy evolves: molecules have a clear preference to adsorb first on the metal surface, then on defects on the NaCl layer, next on the first layer of molecules, and finally on the defect-free NaCl. The electronic π systems of the molecular species are probably responsible for this behavior; they lead to high interaction energy with the electron rich metal surface and with locally modified charge densities around defects in the NaCl layer, and to a lesser extent, with other aromatic π systems. As a consequence, the perspectives of fabricating bimolecular wires and ribbons on defect-free NaCl layers seem rather poor. However, in the next sections, we will see how the use of a vicinal surface significantly modifies the growth scenario.

3.3. Growth of NaCl on the vicinal Au(11 12 12) surface

Fig. 4a shows the surface topography resulting from a deposit of NaCl on a Au(11 12 12) surface held at low-temperature ($T \sim 95$ K). The Au(11 12 12) surface has characteristic 5.8 nm wide Au(1 1 1) terraces separated by straight monatomic steps and periodic truncated "V"-shape discommensuration lines present at the border between face-centered cubic (fcc) and hexagonal close-packed (hcp) stacking domains [25]. NaCl nucleates at the lower part of step edges where fcc stacking regions are wider. On azimuthally slightly disoriented Au(6 6 7) surfaces, it has been observed [26] that these locations of the step edge are prone to contain kinks. As will be shown below it is most likely that such kinks are the nucleation sites of NaCl islands. 1 ML NaCl islands with mostly straight edges and a significant amount of kinks cover the fcc stacking regions of the lower terrace. If 1 ML NaCl islands become larger than the terrace width, the growth continues, most commonly, at the upper part of the step edge, and coalescence can take place between islands from different terraces. Most 1 ML NaCl islands exhibit apolar edges rotated by 45° with respect to the Au(11 12 12) step edge direction, which corresponds to an alignment of the polar axis of the NaCl structure along the Au step edge direction (see type-A orientation in Fig. 4b). The preference for such a configuration might be explained by the interaction of the particular spatial charge distribution at steps of the metal surface and that of the ionic NaCl islands: parallel to the polar NaCl axis there are alternating rows with negative and positive charge. Along the steps, there is a charge distribution with positive and negative charge along the upper and lower part of the step edge, respectively [27]. Accordingly, we expect the step bottom to allocate a line of Na^+ atoms and the overlayer adapts so that the juxtaposed Cl^- row of atoms lays on the upper part of the step.

Occasionally, 2 ML NaCl islands are observed. In contrast to 1 ML islands, they can grow with the apolar axis of the NaCl structure parallel to the Au steps (type-B orientation in Fig. 4b). Post-annealing of the sample to 315 K allows NaCl diffusion along and over step edges, resulting in a significant decrease of the island density (not shown). After annealing to 325 K, the number of islands is further reduced (ripening). This reduction is not due to desorption of NaCl which occurs at 550 K, but to a partial transformation of 1 ML into 2 ML islands (Fig. 4c). This interpretation is not only deduced from the analysis of line profiles – the apparent heights are (2.0 ± 0.2) Å and (3.0 ± 0.2) Å for 1 and 2 ML islands, respectively – but also from the observation of two distinct

contour shapes. 1 ML and most of the 2 ML NaCl islands present edges following the apolar axis of NaCl layers. For 1 ML islands, however, the two equivalent apolar axes (rotated by 90° with respect to each other) alternate frequently, which results in an apparent overall elliptic island shape. We observe that edges of 2 ML islands are straighter than those of 1 ML islands (highlighted

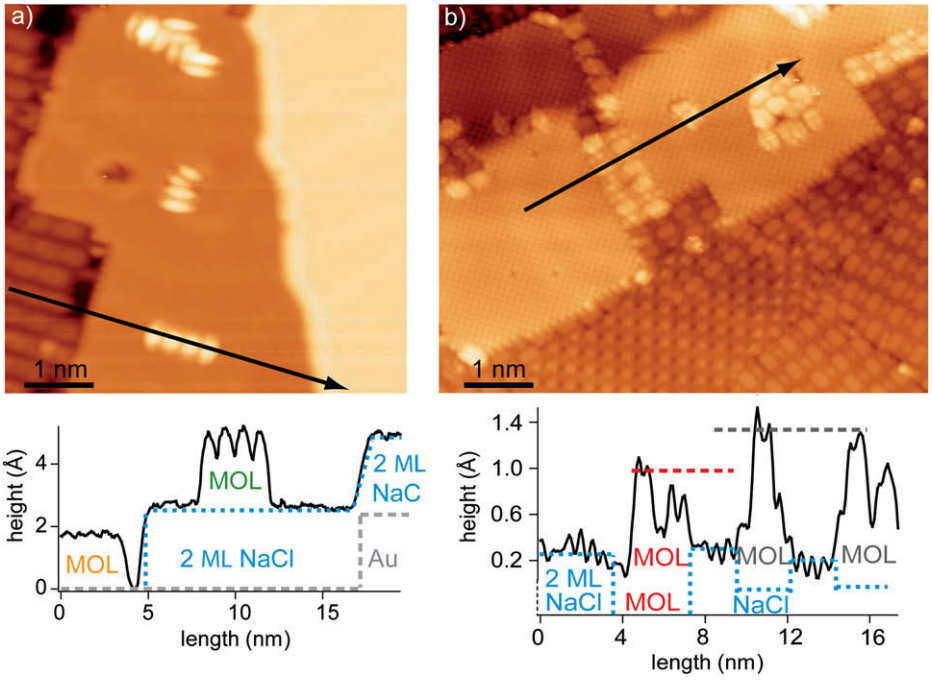

Fig. 3. STM images showing molecular structures resulting from codeposition of PTCDI and BDATB on a partially NaCl-covered Au(1 1 1) surface. (a) Most of the imaged area are 2 ML high NaCl islands apart from the left hand side showing the bimolecular layer on Au(1 1 1). Some molecules are found to adsorb on the NaCl islands – most likely at defects within the salt layer. Under the line profile we indicate the chemical composition of the surface using the following colour code: yellow: molecules adsorbed on Au, green: molecules adsorbed on a 2 ML NaCl island. (b) After an additional bimolecular deposit, PTCDI and BDATB prefer to form a second molecular layer on the bimolecular domains rather than to adsorb on the NaCl islands. Only square shaped pits within the NaCl layer are filled by molecules. The line profile shows the difference in apparent height (of about 0.4 Å) between PTCDI molecules within a bimolecular double-layer (red) and PTCDI molecules adsorbed on a single-layer of NaCl (grey). (For interpretation of the references to colour in this figure legend, the reader is referred to the web version of this article.)

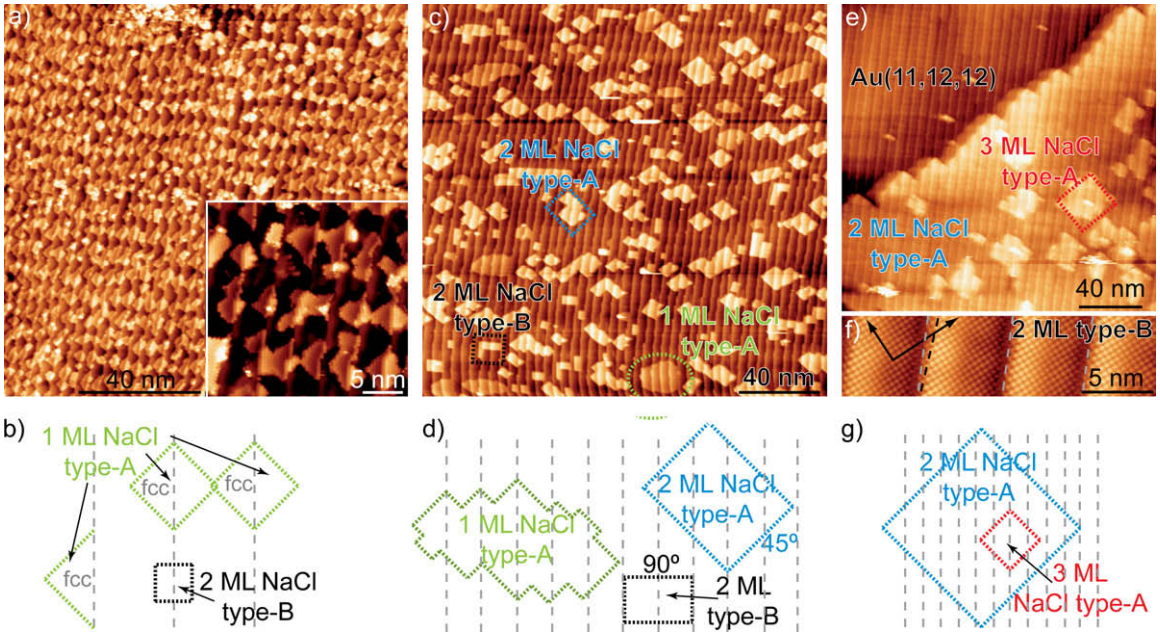

Fig. 4. STM images showing the structural evolution of NaCl islands on Au(11 12 12) upon annealing (a,c,e) and corresponding schemes (b,d,g). (a) Deposition at 95 K leads to the formation of a periodic array of small single-layer NaCl islands ($V = -1.5$ V, $I = 0.08$ nA). The inset shows preferred nucleation at fcc stacking areas of the Au(11 12 12) surface ($V = -1.5$ V, $I = 0.08$ nA). (b) Scheme of the NaCl island orientation and thickness in (a). Dashed grey lines indicate Au step edges. (c) Annealing of the surface shown in (a) to 325 K results in the formation of double-layer islands, giving the impression of a reduced NaCl coverage ($V = -1.9$ V, $I = 0.07$ nA). Dotted lines highlight double (blue and black) and single (green) layer islands. (d) Scheme of the NaCl island orientation and thickness in (c). (e) Surface structure after a high coverage NaCl-deposit at 350 K ($V = 1.0$ V, $I = 0.05$ nA). (f) Atomic resolution of a type-B NaCl bilayer across four terraces ($V = -0.04$ V, $I = 0.06$ nA). (g) Scheme of the NaCl islands' orientation and thickness in (e). (For interpretation of the references to colour in this figure legend, the reader is referred to the web version of this article.)

with dotted blue and black, and dotted green lines, respectively, in Fig. 4c and schematically represented in Fig. 4d). We suggest this to be caused by the orientational organization of dipole moments, which has been commented on above for the NaCl/Au(1 1 1) system. In contrast to the case of Au(1 1 1), the Au(11 12 12) surface provides significantly straighter steps, favoring certain NaCl island orientations more strongly than a meandering step would do. A study of the abundance of island types (after the mentioned annealing at ~325 K) taking into account the thickness and the orientation, reveals that the nucleation of 2 ML NaCl islands with apolar edges oriented by 45° (type-A) or by 90° (type-B) away from the step is equally favourable (47% and 42% occurrence, respectively). Type-A islands are, however, significantly larger than type-B islands (3.8 times larger surface area), indicating that there is a preference for having the apolar NaCl axis oriented along the step. After annealing, 1 ML NaCl islands are relatively sparse (10% occurrence), but their surface area is on average 1.8 times larger than that of A-type 2 ML NaCl islands.

Fig. 4e shows the surface topography after a deposit of NaCl with the sample held at 350 K. In this case, extended double-layer domains with straight apolar edges coexist with clean metal areas (40% of the surface). For the shown large NaCl island, the polar axis is parallel to the steps (type-A orientation). Smaller square shaped patches of an extra layer (3 ML NaCl) are observed exhibiting an apparent height of (4.0 ± 0.2) Å with respect to the metal (see scheme in Fig. 4g). Fig. 4f shows an atomic resolution image of a B-type 2 ML NaCl island over four substrate terraces. For the overall island, the apolar axis of the ionic layer is coincident with the step edge direction. Locally, however, kinks within the vicinal metal surface must have introduced a deviation of the local step direction from the nominal one, resulting in a slight deviation of the apolar NaCl axis from the local step direction. In Fig. 4f, the estimated step edge position is indicated by dashed grey lines, while both polar axes of the NaCl structure are highlighted by black arrows. The dashed black line indicates the direction of the apolar axis of the NaCl structure.

The orientation of the salt relative to the Au superlattice is locally modified by defects in the step edge structure. Defects such as kinks modify the step's intrinsic dipole, which we suggest to influence the growth of NaCl islands. A kink is an additional monatomic step in a different direction, thus the dipoles originating from the Smoluchowski effect are expected to be even more pronounced. Kinks might thus take two different roles: They present preferential nucleation sites – as suggested from LT NaCl-deposit results – leading to the growth of several orientational domains, and they lead to local elastic deformations of the NaCl(0 0 1) plane.

3.4. Bimolecular ribbons on NaCl/Au(11 12 12)

NaCl/Au(11 12 12) samples with extended NaCl islands and clean metal regions as seen in Fig. 4e were used as substrates for codeposition of BDATB and PTCDI molecules. Both molecular species exhibit a clear preference to adsorb on the metal, which leads to a complete coverage of the NaCl-free areas with the bimolecular structure observed previously [14] and shown in Fig. 1. As the bimolecular coverage is increased above full metal coverage, heteromolecular intermixed domains also grow on the 2 ML NaCl film (see Fig. 5a). In the present case neither polar nor apolar NaCl axes are oriented along the local step edge direction, which we attribute to a high density of kinks along the steps of the underlying surface in this region,. Interestingly, the bimolecular PTCDI–BDATB lattice does not follow the direction given by the Au(11 12 12) step edges, but the direction of the two apolar axes of the NaCl(0 0 1) plane. This is in contrast to one of the most important observations regarding the formation of PTCDI–BDATB bimolecular wires on the vicinal metal surface, where the step direction imprints the growth direction of the supramolecular structure. Clearly, this orientational guiding by the steps is overruled by the directional adsorption on the NaCl lattice.

In contrast to previous findings on porphyrins deposited on NaCl/Cu(1 1 1) [12], molecules are also adsorbed on 3 ML NaCl islands and form the same bimolecular structure as on the metal and on 2 ML NaCl islands. Their adsorption energy, however, must be lower than on 2 ML NaCl, as evidenced by the increased difficulty of scanning such regions, where molecules are frequently displaced due to tip-molecule interactions. In contrast to this, the almost complete bimolecular decoration of the edges of 3 ML NaCl islands identifies them as preferential binding sites (marked with dotted yellow lines in Fig. 5). Molecules adsorbed at such sites (molecular species alternate here as well) show a preference to bind with their long axis perpendicular to the edge. We suggest that the charge distribution along the end groups of the molecular species, with alternated sign due to the nature of the functionalities, complement the alternating sign of the charge distribution along the NaCl edges due to Na^+ and Cl^- ions. However, these molecules anchored at NaCl island edges do not influence the overall growth direction of bimolecular domains.

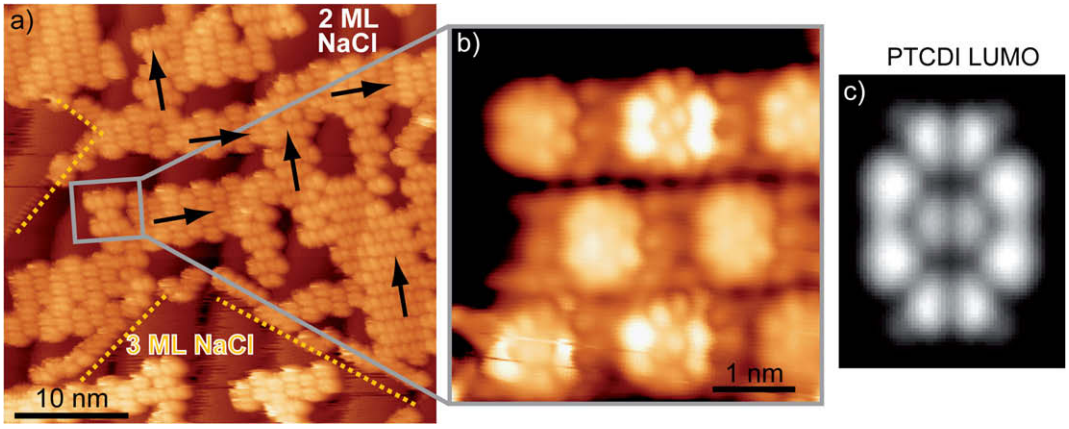

Fig. 5. STM images of BDATB–PTCDI heteromolecular assemblies on NaCl/Au(11 12 12). (a) Bimolecular ribbons adsorbed on double-layer NaCl islands. Black arrows indicate the two row orientations which are along the ⟨1 0 0⟩-directions of the underlying NaCl thin film, as determined from atomic resolution imaging. Dotted yellow lines indicate edges of 3 ML NaCl patches decorated by molecules. On the third layer only few adsorbed molecules are observed (V = 1.9 V, I = 0.05 nA). (b) High resolution image of a bimolecular ribbon adsorbed on 2 ML NaCl. Intramolecular features of the two molecular species are well identified (V = 1.0 V, I = 0.05 nA). (c) Representation of the LUMO of an isolated PTCDI molecule as calculated with Extended Hückel theory. The efficient decoupling of molecular states from the metal substrate is evidenced by the excellent agreement with features of the PTCDI STM images. (For interpretation of the references to colour in this figure legend, the reader is referred to the web version of this article.)

The STM image presented in Fig. 5b resolves the internal molecular structure of a bimolecular domain adsorbed on 2 ML NaCl. The experimentally observed intramolecular features of PTCDI correspond very well to the lowest unoccupied molecular orbital (LUMO) calculated for an isolated PTCDI molecule (Fig. 5c). This evidences very good decoupling of the molecular electronic structure from the metal states by the NaCl layer [28]. Finally, we would like to mention that reliable STS measurements on PTCDI–BDATB molecular assemblies on NaCl islands were not possible due to insufficient stability of the molecular systems.

In summary, small bimolecular PTCDI–BDATB islands are successfully formed on ultrathin NaCl films. However, the targeted superlattice of bimolecular wires – as achieved on the metallic Au(11 12 12) surface [14] – is not observed on NaCl/Au(11 12 12). The step edges of the underlying vicinal Au(11 12 12) surface do not anymore guide the growth direction of bimolecular wires through the NaCl films, which we attribute to the morphological - and probably also electronic - smoothing induced by the NaCl film. Bimolecular PTCDI–BDATB rows orient instead along the apolar axis direction of the NaCl film.

4. Conclusions

Growth and characterization of two-dimensional ordered supramolecular structures on ultrathin NaCl films has only been achieved in very few studies [11–13], which is due to experimental difficulties related to the low molecular adsorption energy on such insulating layers. All three mentioned studies were performed on NaCl islands having similar morphological characteristics as the ones observed here on Au(1 1 1). Our present results suggest a strategy to increase the adsorption energy of molecules on NaCl layers by using a vicinal metal surface, rather than a low index one. On vicinal surfaces with their regularly spaced steps, the characteristic carpet-like step overgrowth of the NaCl layer leads to slight deformations of the NaCl lattice. We propose the correspondingly modified electronic structure of the periodically distorted NaCl layer to be responsible for the enhanced molecular adsorption energy.

We believe that ultrathin insulating layers on vicinal surfaces can be useful for many other studies where an insulating layer between adsorbed molecules and the metal surface is needed. We suggest that other patterned metallic and semiconductor surfaces might lead to a slight deformation of the ionic carpet-like NaCl overlayer, and thus might provide a periodic superlattice of preferential binding sites on the insulator layer.

Note added in proof

After the submission of this paper a STM study of NaCl multilayer islands grown on Au(111) was published [29].

Acknowledgments

We gratefully acknowledge financial support from the European Commission (NMP3-CT-2004-001561 RADSAS) and from the Swiss National Science Foundation (NCCR Nanoscale Science).

References

[1] N. Koch, S. Duhm, J.P. Rabe, A. Vollmer, R.L. Johnson, Phys. Rev. Lett. 95 (2005) 237601.
[2] I. Fernandez-Torrente, S. Monturet, K.J. Franke, J. Fraxedas, N. Lorente, J.I. Pascual, Phys. Rev. Lett. 99 (2007) 176103.
[3] S. Masuda, Y. Koide, M. Aoki, Y. Morikawa, J. Phys. Chem. C 111 (2007) 11747.
[4] X.H. Qiu, G.V. Nazin, W. Ho, Science 299 (2003) 542.
[5] X.H. Qiu, G.V. Nazin, W. Ho, Phys. Rev. Lett. 92 (2004) 206102.
[6] G. Mikaelian, N. Ogawa, X.W. Tu, W. Ho, J. Chem. Phys. 124 (2006) 131101.
[7] K.J. Franke et al., Phys. Rev. Lett. 100 (2008) 036807.
[8] J. Repp, G. Meyer, S.M. Stojkovic, A. Gourdon, C. Joachim, Phys. Rev. Lett. 94 (2005) 026803.
[9] C.J. Villagomez, T. Zambelli, S. Gauthier, A. Gourdon, C. Barthes, S. Stojkovic, C. Joachim, Chem. Phys. Lett. 450 (2007) 107.
[10] P. Liljeroth, J. Repp, G. Meyer, Science 317 (2007) 1203.
[11] A. Scarfato, S.-H. Chang, S. Kuck, J. Brede, G. Hoffmann, R. Wiesendanger, Surf. Sci. 602 (2008) 677.
[12] L. Ramoino, M. von Arx, S. Schintke, A. Baratoff, H.-J. Güntherodt, T.A. Jung, Chem. Phys. Lett. 417 (2006) 22.
[13] E. Cavar, M.-C. Blüm, M. Pivetta, F. Patthey, M. Chergui, W.-D. Schneider, Phys. Rev. Lett. 95 (2005) 196102.
[14] M.E. Cañas-Ventura, W. Xiao, D. Wasserfallen, K. Müllen, H. Brune, J.V. Barth, R. Fasel, Angew. Chem. Int. Ed. 46 (2007) 1814.
[15] I. Horcas, R. Fernández, J.M. Gómez-Rodriguez, J. Colchero, J. Gómez-Herrero, A.M. Baro, Rev. Sci. Instrum. 78 (2007) 013705.
[16] K. Glöckler, M. Sokolowski, A. Soukopp, E. Umbach, Phys. Rev. B 54 (1996) 7705.
[17] W. Hebenstreit, J. Redinger, Z. Horozova, M. Schmid, R. Podloucky, P. Varga, Surf. Sci. 424 (1999) L321.
[18] R. Bennewitz, M. Bammerlin, M. Guggisberg, C. Loppacher, A. Barato, E. Meyer, H.-J. Güntherodt, Surf. Interface Anal. 27 (1999) 462.
[19] S. Fölsch, A. Helms, S. Zöphel, J. Repp, G. Meyer, K.H. Rieder, Phys. Rev. Lett. 84 (2000) 123.
[20] J. Repp, S. Fölsch, G. Meyer, K.-H. Rieder, Phys. Rev. Lett. 86 (2001) 252.
[21] S. Fölsch, A. Riemann, J. Repp, G. Meyer, K.H. Rieder, Phys. Rev. B 66 (2002) 161409.
[22] J. Kramer, C. Tegenkamp, H. Pfnür, J. Phys.: Condens. Matter 15 (2003) 6473.
[23] Note that the apparent height values can only be compared within the same STM image. The values differ substantially depending on tip state or bias voltage used for scanning. This is due to the significant influence of electronic effects on such values.
[24] C. Schwennicke, J. Schimmelpfennig, H. Pfnür, Surf. Sci. 293 (1993) 57.
[25] S. Rousset, V. Rapain, G. Baudot, Y. Garreau, J. Lecoeur, J. Phys.: Condens. Matter 15 (2003) S3363.
[26] F. Leroy, G. Renaud, A. Létoublon, S. Rohart, Y. Girard, V. Repain, S. Rousset, A. Coati, Y. Garreau, Phys. Rev. B 77 (2008) 045430.
[27] R. Smoluchowski, Phys. Rev. 60 (1941) 661.
[28] PTCDI molecules adsorbed on a variety of different metal surfaces have been studied with STM;
see e.g.: C. Ludwig et al., Z. Phys. B 93 (1994) 365;
B. Uder et al., Z. Phys. B 97 (1995) 389;
O. Guillermet et al., Surf. Sci. 548 (2004) 129;
J.C. Swarbrick et al., J. Phys. Chem. B 109 (2005) 12167;
Intramolecular resolution was obtained in some of these cases, but did not show such excellent agreement with calculated molecular orbitals of isolated molecule due to significant interaction with the metal surface.
[29] X. Sun, M.P. Felicissimo, P. Rudolf, F. Silly, Nanotechnology 19 (2008) 495307.